

TEXTURE ANALYSIS IN LD-MOCVD PROCESSED THIN FILM GIANT MAGNETORESISTANT (LaM)MnO₃ MATERIALS

H. GARMESTANI^{a,*}, X. DONG^a, L. BRANDAO^{b,c},
and K.-H. DAHMEN^a

^aMARTECH, Florida State University, Tallahassee, FL 32306-4351,
USA; Mechanical Engineering at FAMU-FSU College of Eng., Tallahassee,
FL 3231, USA; ^bNational High Magnetic Field Laboratory, Tallahassee,
FL 32310, USA; ^cDepartamento de Eng. Mecanica e de Materiais,
IME, Rio de Janeiro, Brazil

(Received 8 October 1999)

Thin films of La_{0.67}Mn_{0.33}MnO₃ (M = Sr), LSMO were deposited on three different substrates of LAO, Sapphire, and Y-ZrO₂ (YSZ) using metal–organic chemical vapor deposition methods. The effect of texture and orientation on the resistance (0 and 6 T) and magnetoresistance (MR) of (LSMO) thin films on various substrates has been investigated. X-ray pole figures were measured using Philips X'Pert X-ray diffractometer equipped with the PopLa analysis package. A direct correlation was observed between the lattice mismatch strain and the structure of the thin film growth. LSMO/LAO seems to be the most perfect system for epitaxial growth due to the negligible lattice-mismatch (~2%). The dominant orientation changes for the films deposited on LAO [100] and LAO [110] substrates while the transition temperature from ferromagnetic to paramagnetic state of the film on LAO [110] is 50 K higher than that of the film on LAO [100]. The MR data and TMI temperature were measured using standard 4-point resistivity devices and SQUID.

Keywords: Epitaxy; Texture measurement; (LaM)MnO₃ GMR films

* Corresponding author. Mechanical Engineering at FAMU-FSU College of Eng., Tallahassee, FL 3231, USA.

INTRODUCTION

Much research has been invested in producing thin film epitaxial GMR (LaM)MnO₃ materials and optimizing their magnetic properties that are critical in applications such as magnetic sensor and recording devices (Petrov *et al.*, 1998; Jin *et al.*, 1994; Hawley *et al.*, 1995). Recent studies on the production of thin film using metal–organic chemical vapor deposition methods (MOCVD) (Dahmen *et al.*, 1997a,b; Gillman *et al.*, 1997) have revealed that the microstructure and the consequent property of the film material depends on the substrate and the deposition parameters. More recently it was shown that the preferred orientation (texture) of the thin film also depends on the type of the substrate and its orientation (Li *et al.*, 1998). Lattice mismatch is one of the most important parameters in this process. In an earlier study (recent work, Weaver *et al.*), we have described texture development and critical thickness of LCMO films on LAO, MgO and YSZ substrates. In this paper more careful investigation of texture development for polycrystalline thin films have been performed for a carefully selected number of substrates of varying lattice mismatch. In this investigation the thin film material chosen is La_{0.67}Sr_{0.33}MnO₃ with a lattice constant of 3.882 Å. The structure of this composite is believed to have monoclinic symmetry at low temperatures and the β angle becomes closer to 90° as the fraction of Sr increases (Hashimoto, 1987).

EXPERIMENTAL PROCEDURE

Thin films of lanthanum manganites were deposited by metal–organic chemical vapor deposition (MOCVD) on three different types of substrates of [100] oriented yttrium stabilized zirconia (YSZ), and LaAlO₃ (LAO) with two orientations of [100] and [110] and Sapphire oriented at [0001] (Table I). A liquid delivery vaporization system (NZ-Applied Technologies) was used to deliver the 2,2,6,6-tetramethyl-3,5-heptanedionato (TMHD) organometallic precursors, La(TMHD)₃, Mn(TMHD)₃, and Sr(TMHD)₂, which were diluted in 25 ml of freshly distilled solvent (diglyme) and vaporized ($T = 250^\circ\text{C}$) at rates of 0.33 and 1.66 $\mu\text{l}/\text{min}$. The gaseous mixture was then introduced to an EMCORE reactor. The substrates were held at a temperature of 700°C

TABLE I *d*-Spacing and lattice mismatch for the film of $(\text{La}_{0.67}\text{Mn}_{0.33})\text{MnO}_3$ films deposited on various substrates $\text{MR} = [R(0) - R(5T)]/R(0)$

Film/substrate	<i>d</i> -Spacing (Å)	Lattice mismatch (%)	Resistance (Ω)	<i>T</i> (<i>MI</i>) (K)	MR% (max)
$\text{La}_{0.67}\text{Sr}_{0.33}\text{MnO}_3/\text{LaAlO}_3$ [100]	3.8833 <100>	2.321	330	362	37
$\text{La}_{0.67}\text{Sr}_{0.33}\text{MnO}_3/\text{LaAlO}_3$ [110]	2.7412 <110>	2.308	880	339	27
$\text{La}_{0.67}\text{Sr}_{0.33}\text{MnO}_3/\text{sapphire}$ [0001]	2.7343 <110>	26.739	14 000	200	—
$\text{La}_{0.67}\text{Sr}_{0.33}\text{MnO}_3/\text{YSZ}$ [100]	2.7320 <110>	6.725	13 000	221	30

during the experiment. Nitrogen (100 sccm) was used as a carrier gas and oxygen (300 sccm) and N_2O (500 sccm) served as oxidants. The deposition rate was approximately $15 \text{ \AA}/\text{min}$. The reactor pressure was 5 torr. After deposition the films were slowly cooled under reaction conditions until the susceptor temperature was below 100°C when the substrates were removed from the susceptor.

To investigate texture low angle XRD scans ($Q = 2^\circ$), normal $2\theta/\Omega$ scans and pole figure analysis were conducted on Siemens D-500 and Philips X'Pert MRD diffractometers operated at 40 kV and 50 mA using CuK_α radiation. The pole figure diffractometer was additionally equipped with a graphite monochromator. Incomplete pole figures were obtained using the reflection technique described by Schultz (1949). The resulting data was analyzed via the spherical harmonics method using the PopLA software package (Kallend *et al.*, 1991) from which the complete and inverse pole figures were reconstructed using the spherical harmonics approach.

Experimental Results

The XRD direct pole figures for the thin film material grown on LAO oriented at [110] (Fig. 1) show an oriented growth as evidenced by the presence of only the [011] type reflections in the X-ray scan. This suggests that the film grows as a single crystal. Interestingly enough thin film materials grown on substrates oriented at [100] direction exhibit a dominant orientation of [100] (Fig. 2). This can be explained based on the low lattice mismatch between the thin film and the LAO substrate (LSMO: $a = 3.882 \text{ \AA}$; LAO: $a = 3.792 \text{ \AA}$). This results into a lattice

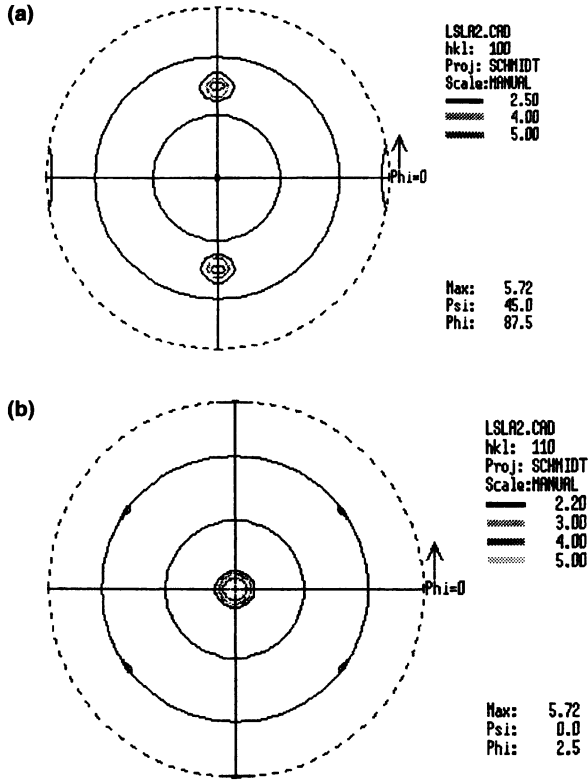


FIGURE 1 $\text{La}_{0.8}\text{Sr}_{0.2}\text{MnO}_3$ thin film grown on LAO [110]. (a) [100] pole figure; (b) [110] pole figure.

mismatch of 2.321% for the LAO [001] and 2.308% for LAO oriented at [011].

The direct pole figures for the thin film materials grown on YSZ oriented at [110] shows evidence for a polycrystalline thin film (Fig. 3). The [100] pole figure shows that the thin film material is axisymmetric with respect to [100] orientation. This suggests that the thin film has grown epitaxially around the dominant orientation. This is verified by an Orientation Distribution Function (ODF) analysis of the pole figure data. The ODF analysis was performed using the three pole figures of [110], [111], and [200]. Inverse pole figures were produced using the ODF data. The inverse pole figure for the normal plane shows that there exists a dominant texture component at $[\bar{2}33]$ orientation (Fig. 4).

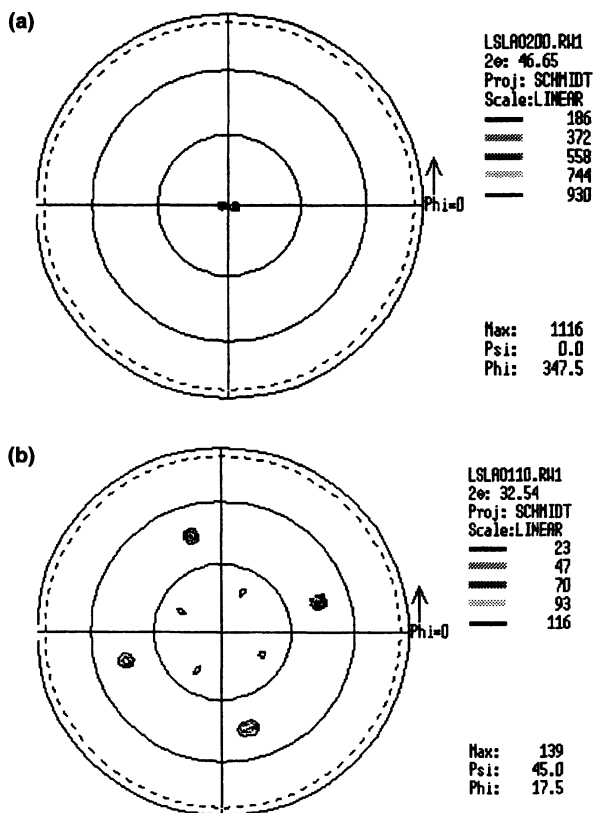


FIGURE 2 $\text{La}_{0.8}\text{Sr}_{0.2}\text{MnO}_3$ grown on LAO [100]. (a) [100] pole figure; (b) [110] pole figure.

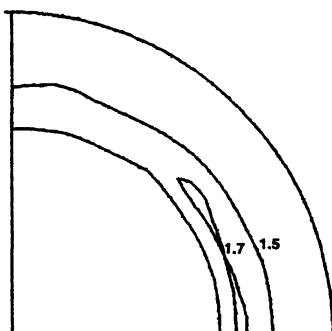


FIGURE 3 Direct (001) pole figure for the LSMO film grown on YSZ oriented at [110].

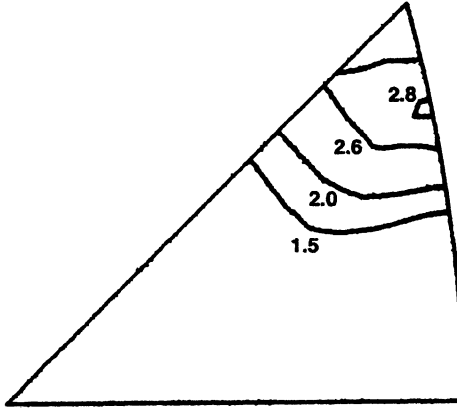


FIGURE 4 Recalculated normal plane inverse pole figure for the LSMO/YSZ.

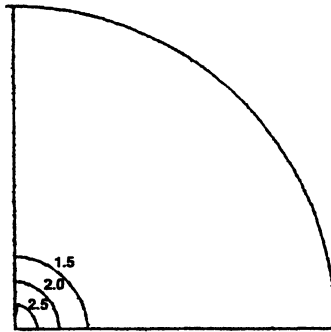


FIGURE 5 Recalculated direct [233] pole figure for the LSMO film grown on YSZ.

The ODF analysis shows a texture intensity of 2.3 times random for this orientation. The recalculated direct pole figure for $[\bar{2}33]$ shows that the polycrystalline thin film grows primarily at this orientation (Fig. 5). The other two in-plane inverse pole figures exhibit a near random texture (a maximum intensity of 1.5 times random). This is more evidence for epitaxial growth.

The direct pole figures for LSMO on Sapphire [0001] shows similar behavior as YSZ (Fig. 6). The ODF analysis was performed using the three pole figures of [100], [110], and [111]. The inverse pole figure for the normal plane direction shows that there are two texture components for the polycrystalline thin film (Fig. 7). One of them shows up at

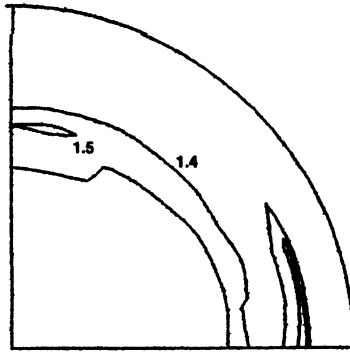


FIGURE 6 Direct (001) pole figure for the LSMO film grown on sapphire oriented at [0001].

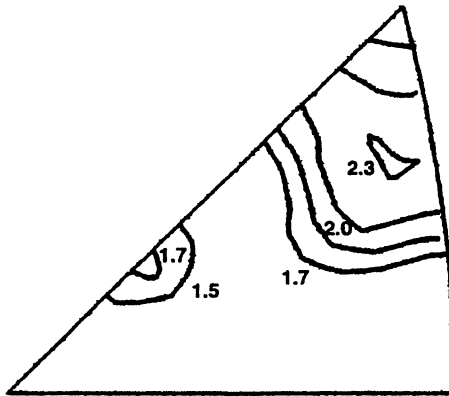


FIGURE 7 Inverse pole figure for the normal plane LSMO/sapphire.

the same orientation as the YSZ substrate, $[\bar{2}33]$ orientation with a texture intensity of 2.7 times random. A direct pole figure in the $[\bar{2}33]$ orientation shows that this is the dominant orientation in the growth of the thin (Fig. 8). The maximum intensity for the two other in-plane inverse pole figures is 1.2, which is evidence for the epitaxial growth. A second weaker texture component also showed up at $[\bar{1}14]$ orientation with a texture intensity of 1.7 times random.

The results of the texture studies can be explained based on the lattice mismatch of the polycrystalline films. The lattice mismatch for the YSZ substrate is 6.7% whereas the one for the Sapphire is 26.7%. The thin

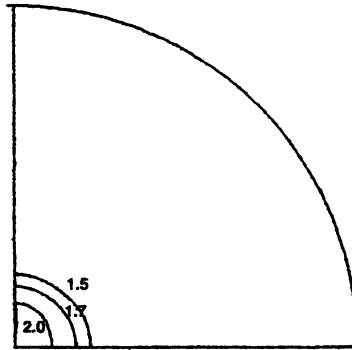


FIGURE 8 Recalculated direct $[233]$ pole figure for the LSMO/sapphire.

film material grown on Sapphire less texture (2.3 compared to 2.7) because of the higher lattice mismatch. A second texture component, $[\bar{1}14]$, also becomes apparent in this film. The thin film deposited on LAO substrate with the lowest lattice mismatch was monocrystalline (or infinitely textured).

The results of this work are correlated to the magnetic property measurements. Epitaxial LSMO [100] and LSMO [110] films on LaAlO_3 (LAO) [100] and [110] substrates show MR ratios which are sharply peaked at the $T(\text{MI})$ (metal-insulator transition). The $T(\text{MI})$ of LCMO [110] is 20 K lower than for LCMO [100] film. The MR value is also slightly smaller for the films on LAO [110] (Table I). Polycrystalline films on Y-ZrO₂ (YSZ) and Sapphire show a nearly constant MR ratio below $T(\text{MI})$.

Due to the polycrystalline nature of the films on SAP [0001] and YSZ [001] a greater resistance is found than with the monocrystalline films on LAO, particularly for $T \ll T(\text{MI})$. The results correlate well with the lattice match of the substrate and the LSMO films: the larger the lattice mismatch the higher the resistance of the film and the lower the $T(\text{MI})$. Similar low temperature MR has recently been observed in both Sr and Ca doped manganites. The proposed explanation for the low temperature MR in polycrystalline films is spin-polarized tunneling at the grain boundaries (Hwang *et al.*, 1996; von Helmolt *et al.*, 1995).

The magnetic anisotropy in thin epitaxially films on LAO [100] and LAO [110] can be interpreted in terms of substrate induced stress. The physics in these CMR materials is governed by an interplay of the Mn e_g

electrons with its double exchange connection to magnetization and the localized effect of strong electron–lattice coupling (Millis *et al.*, 1998; Thomas *et al.*, 1998; Millis, 1998; Suzuki *et al.*, 1997; Jin, 1997; Garcia Munoz *et al.*, 1997). Therefore a uniform compression should increase the electron hopping and reduce the electron–lattice coupling while a uniform biaxial distortion should increase the Jahn–Teller (Goodenough *et al.*, 1961) splitting such that increasingly electrons become more localized. Further investigations are on their way to determine the role of the strain in these CMR materials.

CONCLUSION

The results show that Sapphire substrate with the largest lattice mismatch produce the most polycrystalline thin film material with the lowest texture. Thin films grown on LAO substrate with a lattice mismatch of less than 2.4% resulted in a monocrystalline microstructure. Such results are explained based on the fact that the high lattice mismatch substrates produce a planar defect at the interface and the strain energy due to large lattice mismatch creates a planar defect (microplasticity, dislocation structure, . . .) which can alleviate local stresses. Differences in the MR can be attributed to grain boundary effects and to strain.

Acknowledgements

This work was supported by a grant through the Center for Materials Research and Technology (MARTECH) at Florida State University by DARPA and the Office of Naval Research under contract ONR-N00014-96-1-0767.

References

- Dahmen, K.-H. and Carris, M.W. (1997a) *Chemical Vapor Deposition (Advanced Materials)*, 3, 27–30.
- Dahmen, K.-H. and Carris, M.W. (1997b) *Journal of Alloys and Compounds*, 251, 270–277.
- Garcia Munoz, J.L., Suaaidi, M. and Ritter, C. (1997) *Physica B*, 234, 854–855.
- Gillman, E.S., Carris, M., Smith, C., Dahmen, K.-H., Allendorf, M.D. and Bernard, C. (Eds.) (1997) *Fourteenth International Conference and EUROCVI-11*, NJ (The Electrochemical Society, 1997).

- Goodenough, I.B., Wold, A., Arnott, R.I. and Menyuk, N. (1961) *Physical Review*, **124**(2), 373–384.
- Hashimoto, T. (1987) *J. Cryst. Growth*, **84**, 207.
- Hawley, M.E. *et al.* (1995) *Proc. Symp. Mater. Res. Soc.*, **401**, 531.
- Hwang, H.Y., Cheong, S.W., Ong, N.P. and Batlogg, B. (1996) *Phys. Rev. Lett.*, **77**, 2041.
- Jin, S. *et al.* (1994) *Science*, **264**, 413.
- Jin, S. (1997) *Jom-Journal of the Minerals Metals and Materials Society*, **49**, 61–63.
- Kallend, J., Kocks, U.F., Rollett, A.D. and Wenk, H.-R. (1991) *Materials Science and Engineering A*, **132**, 1–11.
- Li, M. *et al.* (1998) *Residual Stress and Texture in LD-MOCVD Processed Thin Film Giant Magneto-resistant (LaM)MnO₃ Materials*, D. Hui (Ed.), ICCE/5-International Committee on Composite Engineering, Las Vegas, 1998.
- Millis, A.J., Darling, T. and Migliori, A. (1998) *Journal of Applied Physics*, **83**, 1588–1591.
- Millis, A.I. (1998) *Philosophical Transactions of the Royal Society of London Series, a Mathematical Physical and Engineering Sciences*, **356**, 1473–1478.
- Petrov, D.K., Gupta, A., Kirtley, J.R., Krusin-Elbaum, L. and Gill, H.S. (1998) *Journal of Applied Physics*, **83**, 7061–7063.
- Schultz, L.G. (1949) *Journal of Applied Physics*, **20**, 1030.
- Suzuki, Y., Hwang, H.Y., Cheong, S.W. and van Dover, R.B. (1997) *Applied Physics*, **71**, 140–142.
- Thomas, K.A. *et al.* (1998) *Journal of Applied Physics*, **84**, 3939–3948.
- von Helmolt, R., Wecker, I., Samwer, K. and Barner, K. (1995) *J. Mag. Mag. Mat.*, **151**, 411.
- Weaver, M., Brandao, L., Gillman, E.S., Dahmen, K.H. and Garmestani, H. (1999) *Journal of Materials Research*, **14**(5), 2001–2007.